Animal Nutrition 19 (2024) 104–116

Contents lists available at ScienceDirect

Animal Nutrition

journal homepage: http://www.keaipublishing.com/en/journals/aninu/

Original Research Article

Targeting gut microbiota and metabolism profiles with coated sodium butyrate to ameliorate high-energy and low-protein diet-induced intestinal barrier dysfunction in laying hens

Sasa Miao [a], Jiankui Li [a], Ying Chen [b], Wenyan Zhao [a], Mengru Xu [a], Fang Liu [a], Xiaoting Zou [a], Xinyang Dong [a, *]

[a] Key Laboratory of Animal Feed and Nutrition of Zhejiang Province, Key Laboratory of Animal Nutrition and Feed Science (Eastern of China), Ministry of Agriculture and Rural Affairs, The Key Laboratory of Molecular Animal Nutrition, Ministry of Education, College of Animal Sciences, Zhejiang University, Hangzhou 310058, China

[b] Hangzhou Zhejiang University Animal Hospital Co., Ltd., Hangzhou 310058, China

ARTICLE INFO

Article history:
Received 30 March 2024
Received in revised form
30 May 2024
Accepted 11 June 2024
Available online 27 July 2024

Keywords:
Coated sodium butyrate
Intestinal barrier
High-energy and low-protein
Gut microbiota
Laying hen

ABSTRACT

High energy diets are a risk factor for intestinal barrier damage. Butyrate, a major energy source for intestinal epithelial cells, has been shown to improve barrier dysfunction and modulate the gut microbiota. In this trial, we examined the preventative effect of coated sodium butyrate (CSB) on high-energy and low-protein (HELP)-induced intestinal barrier injury in laying hens, and also worked to determine the underlying mechanisms by an integrative analysis of gut microbiota and the metabolome. A total of 216 healthy 28-week-old Huafeng laying hens were randomly assigned to 3 groups with 6 replicates each: the CON group (normal diet), HELP group (HELP diet) and CH500 group (500 mg/kg CSB added to HELP diet). The duration of the trial encompassed a period of 10 weeks. The results revealed that CSB treatment improved the laying rate and mitigated the detrimental effects on intestinal barrier function and the inflammatory response induced by the HELP diet in laying hens ($P < 0.05$). Microbial profiling analysis revealed that the CSB treatment reshaped the HELP-perturbed gut microbiota and promoted the growth of beneficial bacteria ($P < 0.05$). Untargeted metabolomics analysis revealed that CSB reduced the metabolites associated with intestinal inflammation ($P < 0.05$). In conclusion, CSB did not merely modulate alterations in the gut microbiota composition and microbial metabolites but also yielded increased egg production, while mitigating intestinal barrier dysfunction and inflammatory responses induced by HELP in laying hens.

1. Introduction

Non-alcoholic fatty liver disease (NAFLD) is considered the hepatic manifestation of the metabolic syndrome, emerging as a major worldwide health issue in recent decades (Wang et al., 2018). Multiple references illustrated that altered intestinal barrier function and heightened intestinal inflammation are closely involved in the onset and progression of NAFLD (Rahman et al., 2016; Liu et al., 2023). Regarding events in humans, mice and common carps, intestinal barrier injury can lead to increased mucosal permeability, thereby increasing the likelihood of the translocation of microbes and metabolites, inducing inflammation, an immune response, and hepatocyte injury in NAFLD (Csak et al., 2011; Luther et al., 2015; Miao et al., 2023). Thus, the integrity and function of the intestinal barrier are considered early markers that influence the progression of NAFLD.

Studies have revealed that intestinal microbes and metabolites regulate intestinal barrier structure and function. For instance, the

* Corresponding author.
E-mail address: sophiedxy@zju.edu.cn (X. Dong).

Peer review under the responsibility of Chinese Association of Animal Science and Veterinary Medicine.

Production and Hosting by Elsevier on behalf of KeAi

https://doi.org/10.1016/j.aninu.2024.06.006

potentially beneficial bacteria *Clostridium butyricum* or its metabolite, butyric acid, can protect the epithelial barrier by maintaining the expression of tight junction-related genes such as tight junction protein zonula occludens-1 (*ZO-1*) and occludin, in the intestines of mice (Li et al., 2018). Conversely, an escalation in the population of opportunistic pathogenic bacteria or their metabolites can lead to alterations in intestinal structure and permeability. This heightened permeability allows for microbial interaction with intestinal immune cells, thereby triggering an inflammatory response (Lee, 2015). Additionally, studies have shown that intestine-derived microbes such as *Bifidobacterium*, *Ruminococcus* and *Roseburia* are thought to be associated with the progression of NAFLD (Le Roy et al., 2013; Boursier et al., 2016). Moreover, subsequent investigations revealed that gut microbiota intricately modulates the progression of NAFLD via abundant metabolites, encompassing bile acids, short-chain fatty acids (SCFA), sphingolipids, and lipopolysaccharide (LPS) (Nixon, 2009; Abu-Shanab and Quigley, 2010). These reports corroborate that gut microbes and metabolic phenotypes can be denoted as potential therapeutic targets for ameliorating intestinal barrier injury in NAFLD.

Fatty liver hemorrhage syndrome (FLHS) is a type of hepatic lipid metabolism dysfunction in avian species, bearing significant resemblance to NAFLD in humans (Hamid et al., 2019). The FLHS is known to decrease laying rate and increase mortality in female laying hens (Gao et al., 2019). Intestinal barrier injury can result in heightened translocation of gut materials into blood circulation, followed by an influx of pathogenic bacteria and/or harmful metabolites to other organs, such as the oviduct. Although most of the live bacteria are likely lysed or killed by lysozyme and other antimicrobials in the egg albumen (Gantois et al., 2009), a recent study by Shterzer et al. (2020) suggested that at least bacterial products (such as LPS and microbial DNA), if not live bacteria, might be found in the egg. Considering the demonstrated survival of *Salmonella* in the albumen environment (Schoeni et al., 1995), it would not be surprising if other bacteria exhibited similar resilience. Recent investigations indicate that birds with FLHS experience intestinal barrier injuries, which correlate with the severity of hepatic disorders and disturbances in the intestinal microbiome (Hamid et al., 2019; Gu et al., 2020; Nii et al., 2020). Therefore, intestinal barrier injury in hens with FLHS will not only impact the bird's health but also lead to contaminated eggs, which might cause foodborne diseases in humans. Analogous to the situation in humans, the intestinal micro-environment has an essential role in the progression of FLHS and may be regarded as a prospective therapeutic target for the treatment of liver lipid metabolism disorder in birds. As such, protecting hens from FLHS by targeting gut microbiota and metabolites to ameliorate intestinal barrier injury is becoming an increasingly important strategy.

A growing body of evidence has shown that butyrate, a major energy source for intestinal epithelial cells, is a pivotal regulator of the intestinal micro-environment, exerting influences such as the improvement of barrier dysfunction (Grilli et al., 2016; Nielsen et al., 2018), and the modulation of gut microbiota (Huang et al., 2015). Previous literature also demonstrated the protective effects of butyrate against high-fat diet-induced hepatic steatosis by regulating gut microbiota and enhancing the gastrointestinal barrier function in mice (Zhou et al., 2017). Additionally, our previous work has confirmed that butyrate exhibited the capacity to prevent and treat FLHS by regulating lipid metabolism and autophagy in laying hens (Miao et al., 2024). However, the question of whether butyrate could ameliorate intestinal barrier injury in laying hens with FLHS, and its underlying mechanism, remains unclear. In this study, we hypothesize that the gut microbiota and/or metabolites play a vital role in mediating the positive effect of butyrate on intestinal barrier function in laying hens with FLHS. To investigate this hypothesis, this study first assessed the effect of butyrate (coated sodium butyrate [CSB]) in ameliorating intestinal barrier injury using a high-energy and low-protein (HELP) diet-induced FLHS laying hen model and determined the underlying mechanisms by an integrative analysis of gut microbiota and the metabolome.

2. Materials and methods

2.1. Animal ethics statement

All experimental protocols involving animals were approved by the Animal Care and Welfare Committee of Animal Science College and the Scientific Ethical Committee of Zhejiang University (No. ZJU2013105002) (Hangzhou, China).

2.2. Experimental design, animals, and diet

Following a one-week acclimatization period, 216 healthy 28-week-old Huafeng laying hens were randomly assigned to 3 groups with 6 replicates each, namely, the CON group (normal diet), HELP group (HELP diet) and CH500 group (500 mg/kg CSB added to HELP diet). The CSB (sodium butyrate content was 50% coated with palm oil and silica) was procured from Hangzhou Dade Biotechnology Co. Ltd. (Hangzhou, China). The section on CSB dosage in this experiment was guided by our previous report (Miao et al., 2024), which documented a noteworthy positive impact on ameliorating HELP diet-induced hepatic dysfunction. The trial extended over 10 weeks, during which the hens were provided ad libitum access to both feed and water. The coop underwent disinfection regularly, while ventilation and lighting conditions remained identical, maintaining an average daily light exposure of 16 h. The diet composition of the CON and HELP groups is shown in Table 1. Diet samples were analyzed for dry matter (method 930.15) and crude protein (method 990.03) following the methods of the Association of Official Analytical Chemists (AOAC, 2006), as well as the concentration of amino acids using an amino acids analyzer (L-8900 Hitachi, Tokyo, Japan). Levels of calcium and total phosphorus were ascertained through ethylene diamine tetraacetic acid (EDTA) and ammonium metavanadate colorimetry following the China National standard (GB/T 6436-2018 and GB/T 6437-2018). Metabolizable energy was calculated according to the *Chinese Feed Composition and Nutritional Value Table* (31st edition, 2020), Chinese feed database (Xiong et al., 2020).

2.3. Hen performance and egg quality

Throughout the study, egg production and egg weight were recorded daily, and feed consumption was recorded weekly. After the trial, the laying rate per replicate, average egg weight, average daily feed intake (ADFI), and feed conversion ratio (FCR) were all calculated. At the end of the trial, eggs were collected for the determination of egg quality parameters, and a random sample of 4 eggs was chosen from each replicate. Eggshell strength, Haugh unit, yolk color, and eggshell thickness (without the shell membrane) were measured with a digital egg tester (DET-6000, NABEL, Kyoto, Japan).

2.4. Sample collection

After the trial, 2 birds per repetition were randomly chosen and subjected to a 12 h fasting period. Blood samples were collected from wing veins, then separated by centrifugation (1509 $\times$ *g*), and immediately stored at −80 °C. Portions of the duodenum, jejunum and ileum were removed, immediately rinsed with saline to

Table 1
Composition and nutrient levels of diets (air-dry basis, %).

Item	Normal diet	High-energy and low-protein diet
Ingredients		
Corn	64.50	69.70
Soybean meal	24.00	14.58
Corn oil	0.00	4.22
Limestone	8.00	8.00
$CaHPO_4$	1.20	1.20
NaCl	0.30	0.30
Premix[1]	2.00	2.00
Total	100.00	100.00
Nutrient levels[2]		
Crude protein	15.76	12.02
Calcium	3.43	3.21
Total phosphorus	0.59	0.53
Methionine	0.38	0.33
Lysine	0.76	0.66
Metabolizable energy, kcal/kg	2650.05	2946.00

[1] Premix provided the following per kilogram of diets: Cu 2.50 mg, Fe 20.00 mg, Zn 17.50 mg, Mn 15.00 mg, KI 4.00 mg, Na_2SeO_3 6.00 mg, $CoCl_2 \cdot 6H_2O$ 2.50 mg, Met 50.00 mg, chromium 2.00 mg, multivitamin 15.00 mg, phytase 10.00 mg, kininase 7.50 mg, antioxidant 2.00 mg, betaine 15.00 mg, choline 50.00 mg, zeolite, 76.00 mg.
[2] Metabolizable energy was calculated, while the others were measured.

remove intestinal contents, and fixed in 4% paraformaldehyde and/or 2.5% glutaraldehyde solution. Additionally, the remaining small intestinal tissue was promptly stored at −80 °C for subsequent analyses. The cecal contents were collected for omics analysis.

2.5. Intestinal morphology examination

Hematoxylin–eosin (H&E) staining was employed to assess duodenal, jejunal and ileal tissue morphology in accordance with established protocols (Xu et al., 2023). In brief, 4% paraformaldehyde was utilized to fix the freshly isolated intestine segment. The samples underwent processing involving embedding, sectioning, and staining. Subsequently, images of the duodenal, jejunal and ileal morphology were captured and quantified, including measurements of villus height, crypt depth and villus height to crypt depth ratio (VCR) using the microscope (Media Cybernetics, Inc., Rockville, MD, USA).

The transmission electron microscopy (TEM) experiment adhered to established protocols (Cao et al., 2019). Jejunum samples were initially fixed in 2.5% glutaraldehyde and subsequently treated with 1% OsO_4. Following dehydration, infiltration, embedding, ultrathin sectioning, and staining, images were acquired using transmission electron microscopy (TEM) (Model H-7650, Hitachi, Japan). The processing of samples remained consistent with that employed for scanning electron microscopy (SEM), spanning from the fixation stage to the dehydration steps. The subsequent procedures involved further dehydration, coating, and observation utilizing SEM equipment (Model TM-1000, Philips, Japan).

2.6. Intestinal mucosal permeability

The levels of diamine oxidase (DAO), D-lactate (DL), and LPS in the serum were determined by commercial ELISA kits (JM-09299C1, JM-09310C1 and JM-09242C1, Jiangsu Jingmei Biotechnology, Yancheng, China) according to the manufacturer's protocol.

2.7. Immunofluorescence staining and TUNEL assay

Paraffin-embedded jejunum samples were sectioned into 5-μm slides. Sections underwent a systematic processing regimen according to the previous protocol (Wang et al., 2022) and were incubated with primary and secondary antibodies. After that, the sections were counterstained with 4,6-diamidino-2-phenylindole (DAPI, G1012, Servicebio, Wuhan, China). β-Catenin (dilution 1:100, AF10715, Aifang Biotechnology, Changsha, China), ZO-1 (dilution 1:200, GB111402, Servicebio, Wuhan, China), Occludin (dilution 1:300, SAF009, Aifang Biotechnology, Changsha, China), proliferating cell nuclear antigen (PCNA) (dilution 1:500, AF300029, Aifang Biotechnology, Changsha, China), and F4/80 (dilution 1:500, GB113373, Servicebio, Wuhan, China) were used in this trial.

The TUNEL assay was conducted using the one-step TUNEL apoptosis assay kit (C1088, Beyotime Biotechnology, Shanghai, China) according to the manufacturer's protocol. Images of all the above-processed slides were captured using a confocal microscope (FV 1000; Olympus, Tokyo, Japan), and fluorescence intensity was quantified using Image J software.

2.8. Real-time quantitative PCR (RT-qPCR)

Approximately 50 mg of intestine tissue was used for total RNA extraction, employing 1 mL TRIzol reagent, followed by reverse transcription in accordance with the cDNA synthesis kit instructions (R223, Vazyme, Nanjing, China). RT-qPCR was conducted using the SYBR Green Master Mix (Q711, Vazyme, Nanjing, China) on the Applied Biosystems Quant Studio 3 Real-Time PCR System. The relative mRNA expression of target genes was normalized to that of β-Actin levels using the comparative $2^{-\triangle\triangle Ct}$ method (Livak and Schmittgen, 2001). The primer sequences employed for RT-qPCR are detailed in Table 2.

2.9. Cecal microbiome analysis

Total DNA extraction of microbial communities from cecum samples was performed according to the instructions of the MoBio PowerSoil DNA extraction kit (QIAGEN, NRW, Germany). The V3–V4 regions of the bacterial 16S rRNA gene were targeted for amplification using primers 338F (5′-ACTCCTACGGGAGGCAGCAG-3′) and 806R (5′-GGACTACHVGGGTWTCTAAT-3′). Subsequently, amplified products were purified and subjected to sequencing on an Illumina NovaSeq PE250 platform (Illumina, San Diego, USA), following standard protocols as conducted by Majorbio Bio-Pharm Technology Co. Ltd. (Shanghai, China). Operational taxonomic units (OTU) sharing 97% sequence similarity were grouped, and subsequent data analyses, encompassed alpha diversity, beta diversity, linear discriminant analysis (LDA) effect size (LEfSe), and sample heatmap. Phylogenetic Investigation of Communities by

Table 2
Primer used for real-time quantitative PCR analysis.

Gene	Forward sequence (5′-3′)	Reward sequence (5′-3′)
β-Actin	TCCCTGGAGAAGAGCTATGAA	CAGGACTCCATACCCAAGAAAG
IFN-γ	AGCTGACGGTGGACCTATTATT	GGCTTTGCGCTGGATTC
TNF-α	GACAGCCTATGCCAACAAGTA	TCCACATCTTTCAGAGCATCAA
IL-6	CTCGTCCGGAACAACCTCAA	TCAGGCATTTCTCCTCGTCG
IL-10	CCAGGGACGATGAACTTAACA	GATGGCTTTGCTCCTCTTCT
IL-1β	ACTGGGCATCAAGGGCTA	GGTAGAAGATGAAGCGGGTC
TGF-β1	GATGGACCCGATGAGTATTG	CGTTGAACACGAAGAAGATG
MUC2	CAGCACCAACTTCTCAGTTCC	TCTGCAGCCACACATTCTTT
E-Cadherin	ACTGGTGACATTATTACCGTAGCA	TAGCCACTATGACATCCACTCTGT
ZO-1	TGTAGCCACAGCAAGAGGTG	CTGGAATGGCTCCTTGTGGT
Occludin	TCATCGCCTCCATCGTCTAC	TCTTACTGCGCGTCTTCTGG
Claudin-1	TGGAGGATGACCAGGTGAAGA	CGAGCCACTCTGTTGCCATA
β-Catenin	TGCGAATCAACCCAACAGTA	CTCACCAGCAGACATCAGGA

IFN-γ = interferon-γ; *TNF-α* = tumor necrosis factor-α; *IL-6* = interleukin-6; *IL-10* = interleukin-10; *IL-1β* = interleukin-1β; *TGF-β1* = transforming growth factor beta 1; *MUC2* = mucin 2; *ZO-1* = zonula occluden-1.

Reconstruction of Unobserved States (PICRUSt) was employed to predict functional variations within the intestinal microbiota. The data were analyzed on the RealBio Cloud Platform (http://cloud.Majorbio.com/).

2.10. Untargeted metabolomic analysis

The cecal sample extraction followed the previously established method (Geng et al., 2018). The extracted samples were conducted on a Thermo UHPLC-Q Exactive HF-X system equipped with an ACQUITY HSS T3 column (100 mm × 2.1 mm i.d., 1.8 μm; Waters, USA) at Majorbio Bio-Pharm Technology Co. Ltd. (Shanghai, China). Raw peak extraction, database filtering and calibration of the baseline, peak alignment, deconvolution analysis, peak identification, and integration of the peak area were performed using Progenesis QI (Waters Corporation, Milford, USA) software. Metabolite identification was carried out by querying the Majorbio Database. The resultant data matrix obtained by searching the database was uploaded to the Majorbio cloud platform (https://cloud.majorbio.com) for comprehensive data analysis.

Subsequently, the R package "ropls" (Version 1.6.2) was employed for conducting principal component analysis (PCA) and orthogonal least partial squares discriminant analysis (OPLS-DA), accompanied by a seven-cycle interactive validation to evaluate the stability of the model. Metabolites with Variable importance in the projection (VIP) values exceeding 1 and a significance threshold of $P < 0.05$, as determined by both the OPLS-DA model and Student's *t*-test, were identified as differential metabolites. Differential metabolites between HELP and CSB groups were mapped into their biochemical pathways through metabolic enrichment and pathway analysis based on the KEGG database (http://www.genome.jp/kegg/).

2.11. Statistical analysis

The data were subjected to one-way ANOVA analysis using SPSS 20.0 software, followed by multiple comparisons between groups using Tukey's test. Graphs were generated using GraphPad Prism 8.0 software. All data were expressed as mean and standard error of the means (SEM). $P < 0.05$ were considered statistically significant. Furthermore, Spearman's correlation analysis and Mantel test analysis were constructed using the OmicStudio tools (http://www.omicstudio.com).

3. Results

3.1. CSB increased growth performance and egg quality in laying hens fed with HELP diets

As shown in Tables 3 and 4, compared with the CON group, the HELP diet significantly reduced the laying rate and the eggshell strength ($P < 0.05$), while increasing the FCR ($P = 0.038$). Importantly, CSB treatment conspicuously ameliorated the decline of the laying rate induced by the HELP diets in laying hens.

3.2. CSB repaired intestinal morphology disruption induced by HELP diets in laying hens

As illustrated in Fig. 1A, the duodenal, jejunal, and ileal villi in the HELP group exhibited structural damage and sparse arrangement, while the villi in the CON and CH500 groups were arranged compactly and closely. Additionally, in comparison to the CON group, HELP treatment decreased the villus height and the VCR in the jejunum and ileum ($P < 0.05$), while increasing the crypt depth in the ileum ($P = 0.006$) (Table 5). Nevertheless, the alterations were notably reversed by CSB addition. Subsequently, we evaluated the jejunum microstructure using TEM and SEM. The TEM imaging revealed these phenomena, namely, the jejunal villi were exhibited shortly and sparsely in the HELP group, whereas they were displayed lengthily and densely in the CH500 treatment (Fig. 1B). Similarly, observation using SEM also revealed severe damage, sparsity, shrinkage, and disarray of the jejunal villus in the HELP group, which was ameliorated with CSB addition (Fig. 1C). Finally, we used PCNA labeling for cell proliferation and TUNEL staining to assess apoptosis of the jejunum in laying hens. The immunofluorescence findings revealed that the HELP diet decreased the number of $PCNA^+$ cells ($P < 0.01$), with the crypt cells displaying a dispersed and disordered state; Nevertheless, CSB intervention reversed these anomalies, effectively restoring the proliferative ability of crypt cells (Fig. 1E; Fig. S1A) ($P < 0.01$). Simultaneously, a higher TUNEL fluorescence intensity was observed in the HELP treatment ($P < 0.01$), which was obviously attenuated by the administration of CSB ($P < 0.01$) (Fig. 1D; Fig. S1B).

Table 3
Effects of CSB and HELP on growth performance of laying hens.[1]

Item	CON	HELP	CH500	SEM	*P*-value
Laying rate, %	84.73[a]	76.15[b]	81.18[a]	1.646	<0.001
Egg weight, g	49.37	49.71	49.23	1.323	0.935
ADFI, g	104.97	103.04	105.15	6.353	0.935
FCR	2.32[b]	2.62[a]	2.38[ab]	0.113	0.038

CSB=coated sodium butyrate; HELP=high-energy and low-protein; SEM = standard error of the means; ADFI = average daily feed intake; FCR = feed conversion ratio.
[a,b]Means within a row with different superscripts are significantly different ($P < 0.05$).
[1] CON = normal diet; HELP = high-energy and low-protein diet; CH500 = 500 mg/kg coated sodium butyrate added to high-energy and low-protein diet. Values are represented as the mean and SEM ($n = 6$).

3.3. CSB ameliorated impairment of intestinal epithelial cell junctions induced by HELP diets in laying hens

In Fig. 2A, we tested the mRNA relative expression of tight junction and adherens junction-related genes. The results indicated that the HELP diet obviously decreased the jejunal mRNA relative expressions of β-Catenin ($P < 0.01$), E-Cadherin ($P < 0.01$), *ZO-1* ($P < 0.05$), occludin ($P < 0.05$) and claudin-1 ($P < 0.01$), which was reversed by CSB administration ($P < 0.01$). Furthermore, the protein expression of tight junctions and adherens junctions was verified through immunofluorescence analysis. The resulting images revealed that CSB obviously enhanced the β-Catenin, ZO-1, and occludin fluorescence intensity compared with the HELP group (Fig. 2B). Table 6 displayed that CSB could decrease intestinal permeability, as demonstrated by its effect in decreasing serum

Table 4
Effects of CSB and HELP on egg quality of laying hens.[1]

Item	CON	HELP	CH500	SEM	*P*-value
Eggshell strength, kgf/m^2	4.18[a]	3.59[b]	3.95[ab]	0.157	0.006
Eggshell thickness, mm	0.38	0.37	0.38	0.007	0.079
Haugh unit	79.75	77.73	79.40	2.016	0.577
Yolk color	6.92	6.83	7.00	0.281	0.840

CSB=coated sodium butyrate;HELP=high-energy and low-protein; SEM = standard error of the means.
[a,b]Means within a row with different superscripts are significantly different ($P < 0.05$).
[1] CON = normal diet; HELP = high-energy and low-protein diet; CH500 = 500 mg/kg coated sodium butyrate added to high-energy and low-protein diet. Values are represented as the mean and SEM ($n = 24$).

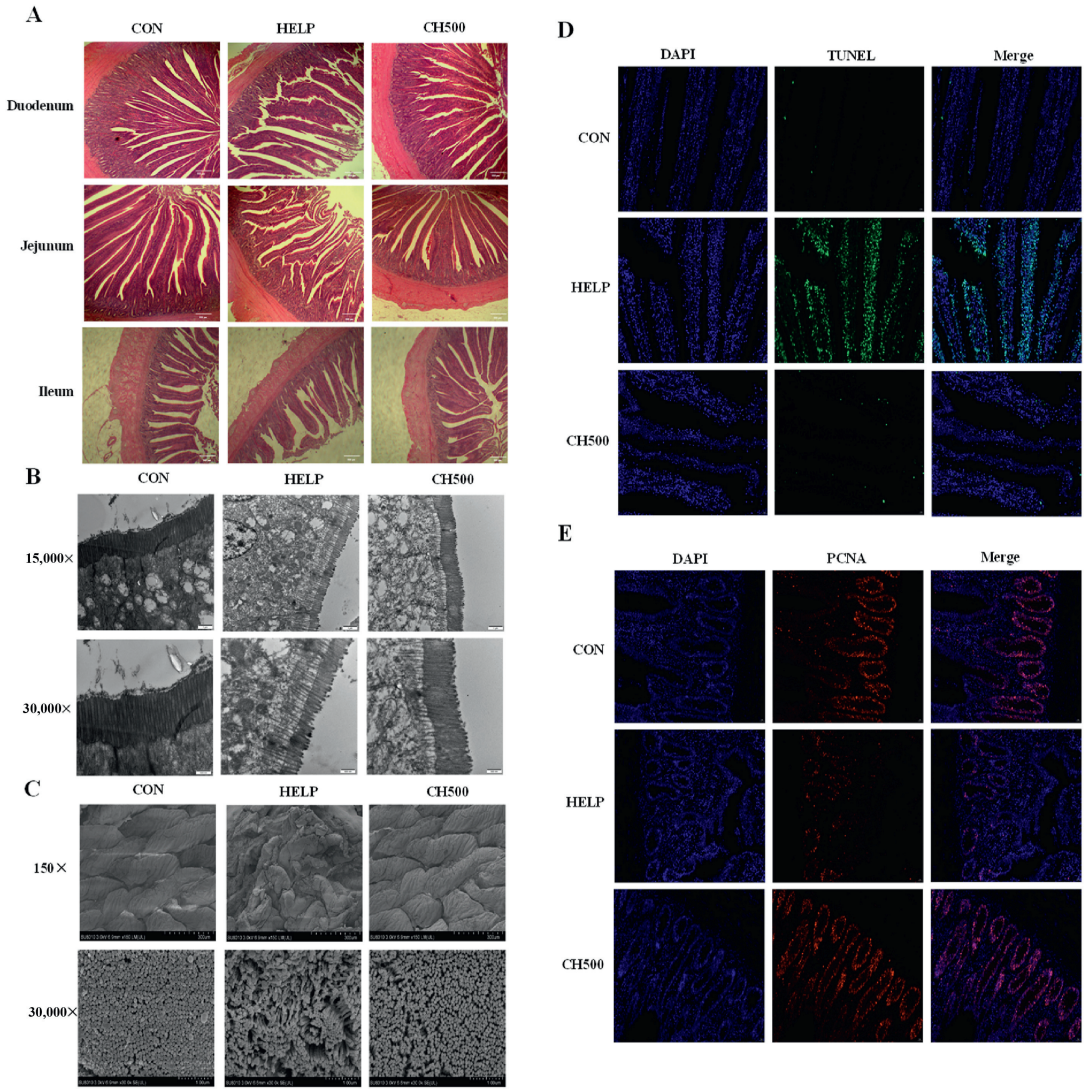

Fig. 1. Coated sodium butyrate (CSB) repaired intestinal morphology disruption induced by high-energy and low-protein (HELP) diets in laying hens. (A) Representative hematoxylin-eosin (H&E)-stained images of duodenum, jejunum and ileum (magnification, 40×). (B) Representative transmission electron microscopy (TEM) images of the jejunum. (C) Representative scanning electron microscopy (SEM) images of jejunum. (D) Representative immunofluorescence images of TUNEL (green) in the jejunum (magnification, 400×). (E) Representative immunofluorescence images of proliferating cell nuclear antigen (PCNA) (red) in the jejunum (magnification, 400×). CON = normal diet; HELP = HELP diet; CH500 = 500 mg/kg CSB added to HELP diet; DAPI = 4′,6-diamidino-2′-phenylindole.

Table 5
Effects of CSB and HELP on villi morphology of small intestine of laying hens.[1]

Item	CON	HELP	CH500	SEM	*P*-value
Duodenum					
Villus height, μm	1284.80	1225.84	1261.38	23.491	0.062
Crypt depth, μm	135.77	143.55	136.53	4.840	0.232
VCR	9.51	8.58	9.12	0.401	0.077
Jejunum					
Villus height, μm	1025.07^{a}	878.43^{b}	973.47^{a}	21.694	<0.001
Crypt depth, μm	98.63^{ab}	107.46^{a}	97.33^{b}	3.536	0.021
VCR	10.44^{a}	8.20^{b}	10.20^{a}	0.391	<0.001
Ileum					
Villus height, μm	796.47^{a}	741.20^{b}	781.42^{ab}	16.960	0.012
Crypt depth, μm	78.45^{b}	90.52^{a}	80.47^{b}	3.471	0.006
VCR	10.22^{a}	8.22^{b}	9.80^{a}	0.523	0.003

CSB=coated sodium butyrate; HELP=high-energy and low-protein; SEM = standard error of the means; VCR = villus height to crypt depth ratio.
^{a,b}Means within a row with different superscripts are significantly different ($P < 0.05$).
[1] CON = normal diet; HELP = high-energy and low-protein diet; CH500 = 500 mg/kg coated sodium butyrate added to high-energy and low-protein diet. Values are represented as the mean and SEM ($n = 12$).

DAO activity, LPS and DL contents compared with the HELP group ($P < 0.05$). These results suggest that CSB has a positive effect for recovering jejunal barrier impairment induced by the HELP diet.

3.4. CSB suppressed excessive intestinal inflammation induced by HELP diets in laying hens

We conducted assessments involving F4/80 fluorescence and the expression of inflammation-related genes. Our data revealed that the HELP diet facilitated the F4/80 macrophage infiltration ($P < 0.01$), but the addition of CSB exhibited a reversal effect on its expression ($P < 0.01$) (Fig. 3A; Fig. S1C). Moreover, CSB administration significantly suppressed interleukin-1β (*IL-1β*) ($P < 0.01$), tumor necrosis factor-α (*TNF-α*) ($P < 0.01$), and interferon-γ (*IFN-γ*) ($P < 0.01$) mRNA expression, and promoted transforming growth factor beta 1 (*TGF-β1*) ($P < 0.01$) and interleukin-10 (*IL-10*) ($P < 0.01$) mRNA relative expression in HELP-treated laying hens, indicating that CSB could attenuate inflammation induced by the HELP diet (Fig. 3B).

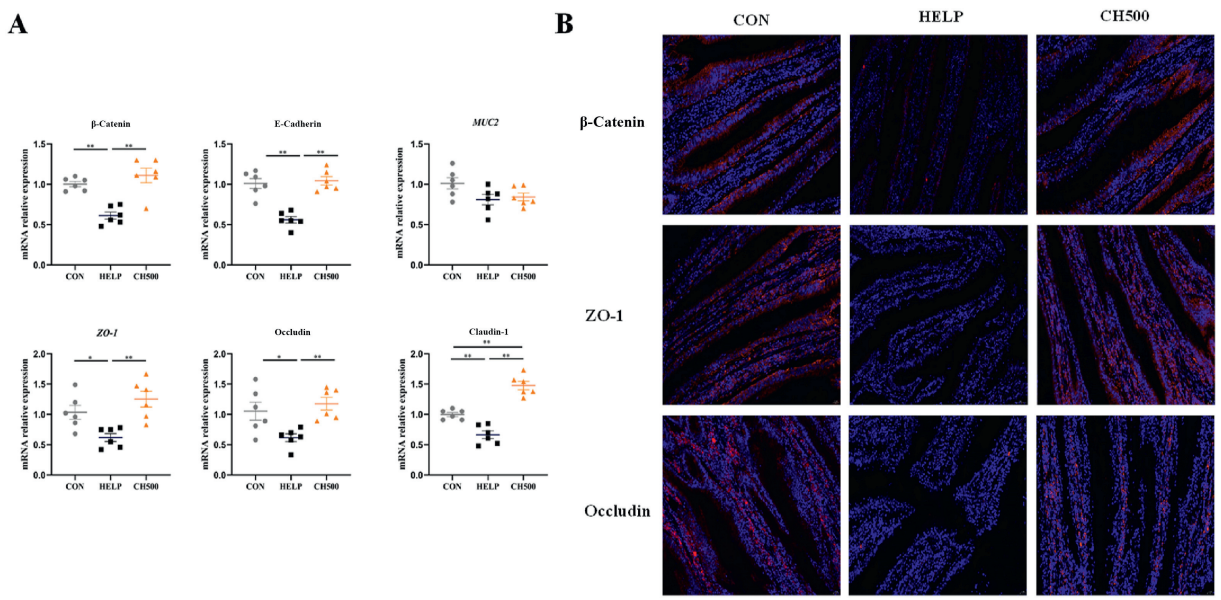

Fig. 2. Coated sodium butyrate (CSB) ameliorated impairment of intestinal epithelial cell junctions induced by high-energy and low-protein (HELP) diets in laying hens. (A) mRNA relative expression of tight junction proteins of jejunum, $n = 6$. (B) Representative immunofluorescence images of β-Catenin (red), ZO-1 (red) and occludin (red) staining in the jejunum (magnification, 400×). CON = normal diet; HELP = HELP diet; CH500 = 500 mg/kg CSB added to HELP diet; *MUC2* = mucin 2; ZO-1 = zonula occluden-1. $^{*}P < 0.05$, $^{**}P < 0.01$.

Table 6
Effects of CSB and HELP on serum indexes of laying hens.[1]

Items	CON	HELP	CH500	SEM	*P*-value
DAO, ng/mL	10.46[b]	15.41[a]	11.04[b]	0.411	<0.001
DL, μg/L	389.48[c]	563.40[a]	437.55[b]	5.507	<0.001
LPS, ng/L	207.11[b]	250.12[a]	213.86[b]	2.774	<0.001

CSB=coated sodium butyrate; HELP=high-energy and low-protein; SEM = standard error of the means; DAO = diamine oxidase; DL = D-lactate; LPS = lipopolysaccharide.
[a–c]Means within a row with different superscripts are significantly different ($P < 0.05$).
[1] CON = normal diet; HELP = high-energy and low-protein diet; CH500 = 500 mg/kg coated sodium butyrate added to high-energy and low-protein diet. Values are represented as the mean and SEM ($n = 6$).

3.5. CSB reshaped gut microbiota changes induced by HELP diets in laying hens

The overall changes in gut microbiota were evaluated by sequencing the 16S rRNA gene of cecum samples isolated from the CON, HELP, and CH500 groups. The rarefaction curves leveled off as the number of sequences increased, indicating sufficient OTU coverage for accurate characterization of microbial composition (Fig. 4A). The Venn diagram highlighted the distinctions in microbiota compositions among these three groups (Fig. 4B). α-Diversity analysis, evaluating species richness and uniformity, revealed a significant increase in the Shannon index ($P < 0.05$) and a decrease in the Simpson index ($P < 0.01$) in the CH500 group compared with HELP group, suggesting that CSB promoted both species richness and uniformity (Fig. 4C). The weighted UniFrac algorithm at the OTU level was used to calculate beta diversity. The PCoA and UPGMA hierarchical clustering analysis displayed that clear separation among the three groups (Fig. 4D and E), indicating that both HELP and CSB induced alterations in the diversity and structure of the intestinal microbiota.

3.6. Species and difference analysis of intestinal flora

To further assess the impact of CSB on the intestinal microbiota in HELP-fed laying hens, this study analyzed the bacterial composition at the phylum and genus level. At the phylum level, Firmicutes and Bacteroidetes were the predominant phyla, followed by Actinobacteriota and Spirochaetota (Fig. 5A). The HELP diet significantly diminished the relative abundance of Firmicutes and enhanced Bacteroidetes abundance, but this change was reversed by CSB administration. *Bacteroides*, *Rikenellaceae_RC9_gut_group*, *Lactobacillus*, and *Romboutsia* were the four predominant genera in each group (Fig. 5B). Subsequently, we employed LEfSe analysis (with an LDA score > 3) to investigate the biomarkers exhibiting significant differences among the three groups (Fig. 5C and D). In the CON group, 13 taxa were identified, 8 taxa in the HELP group, and 11 taxa in the CH500 group. The HELP group exhibited a notable increase in the relative abundance of *Synergistes* and *Rikenellaceae_RC9_gut_group*. CH500 obviously enriched the relative abundance of *Alistipes*, *unclassified_f_Oscillospiraceae*, and *norank_f_Eubacterium_coprostanoligenes_group*. These findings offer evidence that HELP and CSB had an alteration in the composition of the intestinal microbiota.

3.7. Predictive analysis of intestinal flora function

To further explore whether alterations in the structure and composition of the gut flora would induce functional changes, we used PICRUSTs analysis to obtain the KEGG pathway information corresponding to OTU. Subsequently, we calculated the relative abundance of the functional categories of each pathway, and finally obtained the metabolic pathway information at three levels, for which we performed the functional prediction analysis. The analysis results are shown in Fig. 6A, there are six main pathways at level 1, namely, metabolism, genetic information processing, environmental information processing, cellular processes, human

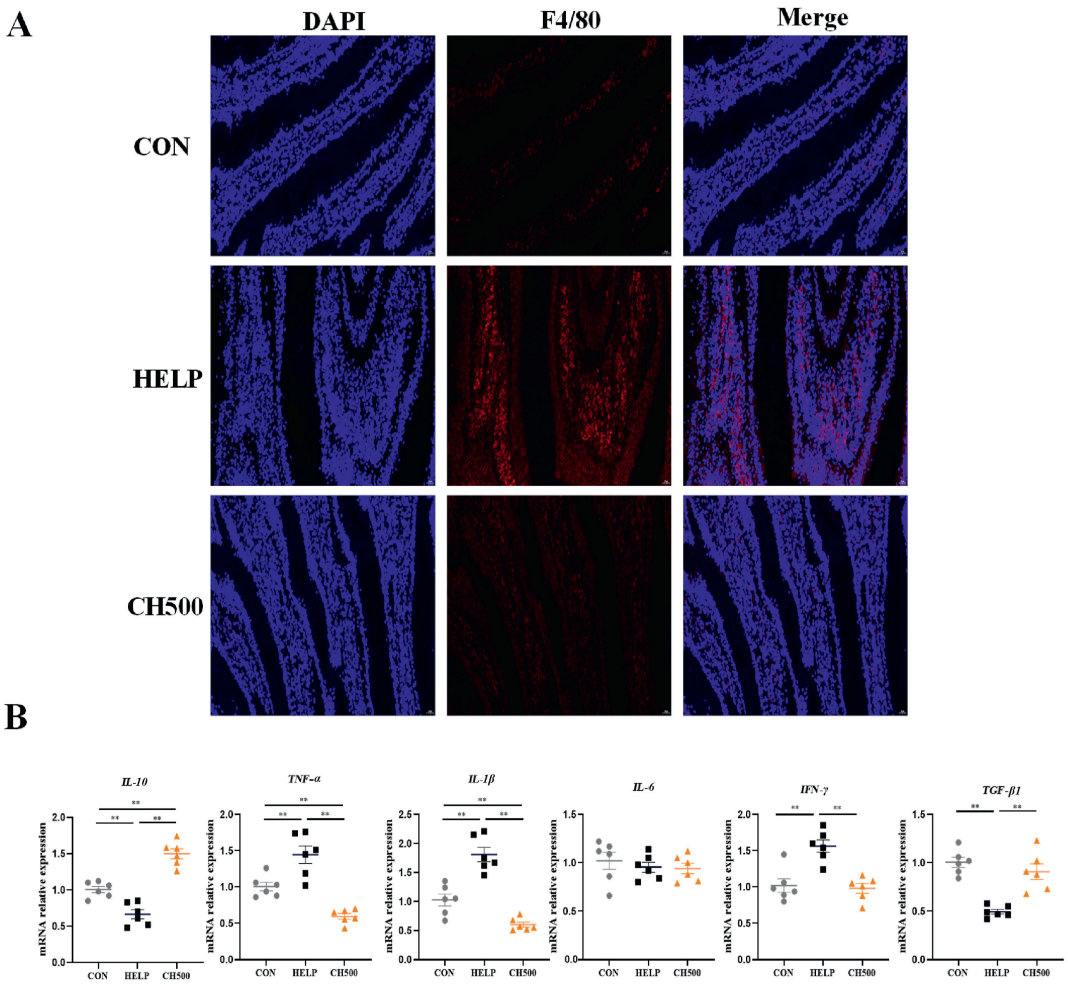

Fig. 3. Coated sodium butyrate (CSB) suppressed excessive intestinal inflammation induced by high-energy and low-protein (HELP) diets in laying hens. (A) Representative immunofluorescence images of F4/80 (red) staining in the jejunum (magnification, 400×). (B) mRNA relative expression of inflammatory cytokines of jejunum, $n = 6$. CON = normal diet; HELP = HELP diet; CH500 = 500 mg/kg CSB added to HELP diet; DAPI = 4′,6-diamidino-2′-phenylindole; *IL-10* = interleukin-10; *TNF-α* = tumor necrosis factor-α; *IL-1β* = interleukin-1β; *IL-6* = interleukin-6; *IFN-γ* = interferon-γ; *TGF-β1* = transforming growth factor beta 1. *$P < 0.05$, **$P < 0.01$.

diseases, and organism systems, among which metabolism is the pathway with the highest proportion at level 1. The results indicated a significant down-regulation of metabolism in the CON and CH500 groups in comparison to the HELP group ($P < 0.01$). Furthermore, cellular processes and environmental information processing were significantly down-regulated in the HELP group in comparison to the CON and CH500 groups. Subsequently, our predictive analysis of gut flora at level 2 revealed that metabolism mainly included carbohydrate metabolism, amino acid metabolism, energy metabolism, metabolism of cofactors and vitamins, and lipid metabolism. Intriguingly, only lipid metabolism pathways exhibited a decrease in the HELP group compared to the CON group (Fig. 6B). To further analyze the specific pathways of lipid metabolism, we analyzed its level 3 level (Fig. 6C), which showed that the linoleic acid metabolism in the CON and CH500 treatment compared to the HELP treatment were significantly decreased; additionally, the arachidonic acid metabolism was decreased in the CH500 treatment compared to the HELP treatment.

3.8. CSB altered the caecal metabolome induced by HELP diets in laying hens

To directly investigate the changes of metabolites in the gut flora, the contents of the cecum were subjected to non-targeted metabolomics analysis using a gas chromatography–mass spectrometry (GC–MS) platform. The PCA, PLS-DA, and OPLS-DA score plots distinctly revealed separated clusters between the two groups, with all samples falling within the 95% confidence interval (Fig. 7A–C). PLS-DA and OPLS-DA were modeled and analyzed with random permutations to verify their validity and robustness (Fig. 7E and F). The results showed that the test parameters of PLS-DA were R2 = (0, 0.9825), Q2 = (0, −0.0331); and OPLS-DA were R2 = (0, 0.9852), Q2 = (0, −0.1509); indicating the authenticity and robustness of the model. According to a VIP > 1 and Student's *t*-test $P < 0.05$, 399 differentially expressed metabolites were screened between the two groups, mainly including lipids, steroids, peptides, hormones and transmitters, among which 25 expressed metabolites were up-regulated, while 374 expressed metabolites were down-regulated (Fig. 7D). Following classification based on similar characteristics, 25 metabolites were definitively recognized as biomarker metabolites (Fig. 7G). Among these, 2,3-dihydroxycarbamazepine exhibited a decrease, whereas 11-HpODE, 9,12,13-TriHOME, 2beta-hydroxytestosterone, 2-n-propyl-4-oxopentanoic acid, 10,11-dihydro xycarbamazepine, prostaglandin B2, and 20-carboxy-leukotriene B4 displayed an increase in the HELP group compared to the CH500 group. Furthermore, KEGG enrichment analysis pinpointed that CSB predominantly influenced linoleic acid metabolism and arachidonic acid metabolism pathways (Fig. 7H).

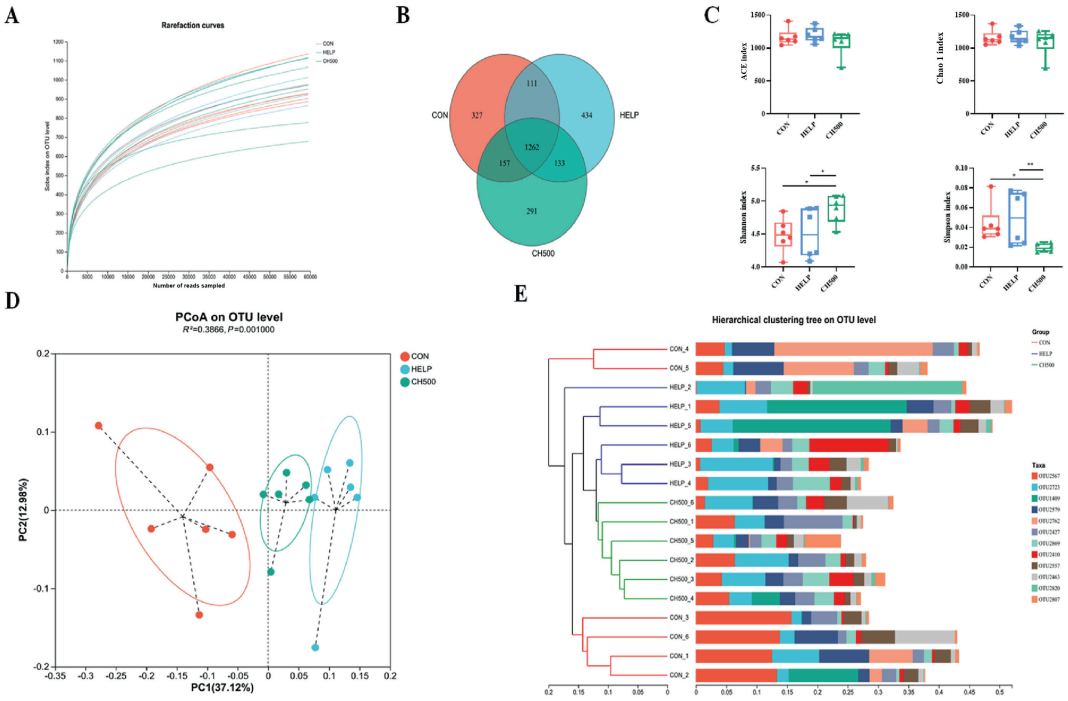

Fig. 4. Richness and biodiversity of cecal flora. (A) Rarefaction curves were determined at the 97% similarity level. (B) Venn diagram of operational taxonomic unit (OTU) in the three groups. (C) α-Diversity indexes of bacterial community. (D) Principal Co-ordinates analysis (PCoA) on OTU level based on weighted UniFrac. (E) Unweighted pair-group method with arithmetic means (UPGMA) hierarchical clustering analysis based on the weighted UniFrac. CON = normal diet; HELP = high-energy and low-protein diet; CH500 = 500 mg/kg coated sodium butyrate added to high-energy and low-protein diet. $^{*}P < 0.05$, $^{**}P < 0.01$.

3.9. Correlation among gut microbiota, metabolites and intestinal barrier related indicators

The potential association between gut microbiota and metabolites was explored through Spearman correlation analysis (Fig. 8A; Fig. S2). Our result displayed that the relative abundance of *norank_f_UCG-010* is negatively correlated with the levels of 9,12,13-TriHOME, 13-L-hydroperoxylinoleic acid, 12-epi-LTB4, (10E,12Z)-(9S)-9-hydroperoxyoctadeca-10,12-dienoic acid, 20-carboxy-leukotriene B4, and 16(R)-HETE; Simultaneously, the relative abundance of *norank_f_Eubacterium_coprostanoligenes_group* is negatively correlated with the levels of 9,12,13-TriHOME, 13-L-hydroperoxylinoleic acid, 12-epi-LTB4, 9-hpode and (10E,12Z)-(9S)-9-hydroperoxyoctadeca-10,12-dienoic acid; the relative abundance of *Sellimonas* is negatively correlated with only the level of 9,12,13-TriHOME. The relative abundance of *Rikenellaceae_RC9_gut_group* is positively correlated with the levels of 12-epi-LTB4, 20-carboxy-leukotriene B4, 16-HETE, prostaglandin G2 and 6-ketoprostaglandin E1. Furthermore, through mantel test analysis (Fig. 8B), strong correlations were observed between intestinal barrier mediators (tight junction proteins, inflammatory factors, and intestinal permeability regulators) and microbiota (genus affiliated with Firmicutes and genus Bacteroidetes), as well as metabolites involved in arachidonic acid and linoleic acid metabolism pathways. Concretely, microbiota demonstrated a strong correlation with the mRNA relative expression of claudin-1, β-catenin, E-catenin, *IL-10*, *TNF-α*, and the levels of DAO, DL, and LPS; meanwhile, metabolites exhibited a strong correlation with the mRNA relative expression of β-catenin, E-catenin, *IL-10*, and *IL-1β*. In addition, the mRNA relative expression of β-catenin, E-catenin, *IL-10*, and *IL-1β* are strongly correlated with both the relative abundance of microbiota and the levels of metabolites.

4. Discussion

The FLHS is tightly connected with decreased egg production in female laying hens, causing great economic losses for the poultry industry (Gao et al., 2019). As such, developing therapeutic approaches to prevent this adverse outcome is becoming important. A HELP diet is linked to an increased incidence of FLHS (Rozenboim et al., 2016). The demonstrated efficacy of CSB in alleviating hepatic steatosis in our previous work (Miao et al., 2024), coupled with its ability to improve productivity of hens fed a HELP diet in the present study, indicates that dietary CSB might be a promising strategy for FLHS treatment in laying hens. It is well established that changes to the integrity and function of the intestinal barrier are considered an early event that influences the initiation and progression of chronic liver disease (Rahman et al., 2016; Liu et al., 2023). However, whether CSB might ameliorate intestinal barrier disruption in laying hens with FLHS remains poorly understood. Thus, the effects of CSB on the integrity and function of the intestinal barrier in HELP diet-induced FLHS laying hens were further evaluated in this study.

The structural integrity is vital to the maintenance of intestinal barrier functions. This study found that the integrity of intestinal architecture was damaged in HELP diet-induced FLHS laying hens. On the one hand, HELP treatment caused intestinal villus atrophy by decreasing the proliferation of crypt epithelial cells and increasing the apoptosis of villi epithelial cells. On the other hand, HELP treatment significantly altered the expression of molecules associated with tight junction and junctional adhesion, including β-catenin, E-cadherin, *ZO-1*, occludin, and claudin-1. Atrophy of villi and loss of tight junction proteins are recognized to elevate intestinal permeability (Jeurissen et al., 2002). As anticipated, markers of intestinal permeability, including DAO, DL, and LPS levels in blood circulation, increased following HELP treatment in the current

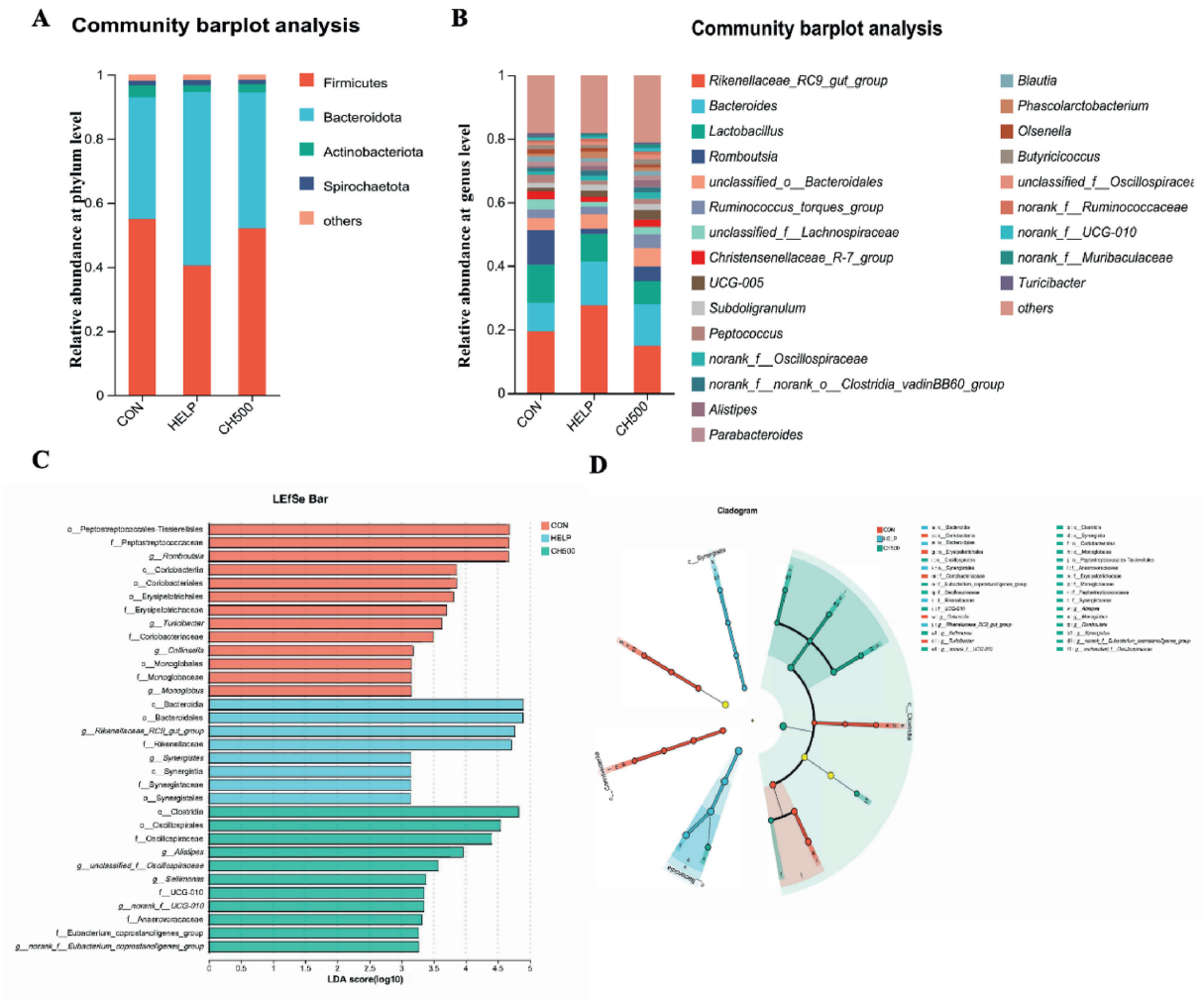

Fig. 5. Species and difference analysis of intestinal flora. (A) Relative abundance of gut microbiota at phylum level. (B) Relative abundance of gut microbiota at genus level. Linear discriminant analysis (LDA) value distribution histogram (C) and cladogram (D) based on LEfSe analysis showed significant differences in the microbial community in the three groups. CON = normal diet; HELP = high-energy and low-protein diet; CH500 = 500 mg/kg coated sodium butyrate added to high-energy and low-protein diet.

study, which further supported the viewpoint that the structural integrity of the intestinal barrier was diminished in laying hens with FLHS. Loss of structural integrity is usually a major cause of inflammatory events in the intestinal mucosa (Capaldo et al., 2017). Consistent with previous observations, HELP treatment in this study did lead to the progression of the inflammatory response, as indicated by increased infiltration of inflammatory cells (F4/80 macrophages), elevated expression of several pro-inflammatory factors (*IL-1β*, *TNF-α*, and *IFN-γ*), and a decrease in anti-inflammatory factors (*TGF-β1* and *IL-10*) in the intestine. The possible molecular mechanisms involved in the pro-inflammatory effects of HELP warrant further investigation in future studies. Nevertheless, the loss of structural integrity and induction of inflammation in the intestinal barrier can not only reduce capacity for nutrient absorption, and hence affect poultry productivity (Nii, 2022), but also permit the translocation of bacteria and bacterial-related products via the mucosa to the whole body, finally resulting in the production of contaminated eggs as described previously (Shterzer et al., 2020). Collectively, our data confirmed that intestinal barrier dysfunction, including damaged structural integrity, increased permeability, and induced intestinal inflammation, could be involved in the development of HELP diet-induced FLHS in laying hens, which is similar to the pathogenetic mechanism of NAFLD in humans (Liu et al., 2023). In accordance with our hypothesis, CSB intervention reversed these anomalies to some extent.

A growing number of data indicates that gut microbiota can be denoted as a promising therapeutic target for ameliorating intestinal barrier dysfunction in diet-induced chronic liver disease, including NAFLD in humans and mice (Boursier et al., 2016; Le Roy et al., 2013), as well as FLHS in birds (Hamid et al., 2019). In this study, HELP diet-induced FLHS laying hens exhibited an elevated relative abundance of Bacteroidetes and a reduced relative abundance of Firmicutes. Similar to our results, previous findings have also observed that chronic liver disease can lead to an imbalance in gut bacteria, with fewer relative abundance of Firmicutes and more Bacteroidetes (Duarte et al., 2019). The CSB intervention reversed the HELP diet-induced changes in the relative abundance of Firmicutes and Bacteroidetes. Firmicutes bacteria, Gram-positive in nature, are responsible for the production of SCFA (Stojanov et al., 2020), which can provide energy for the growth of intestinal epithelial cells, safeguard the structural integrity and function of the intestinal barrier, and suppress the generation of pro-inflammatory factors (Park et al., 2007; Plöger et al., 2012). Conversely, Bacteroidetes bacteria, Gram-negative in nature, have been reported to enhance immune reactions through pro-inflammatory cytokine synthesis via

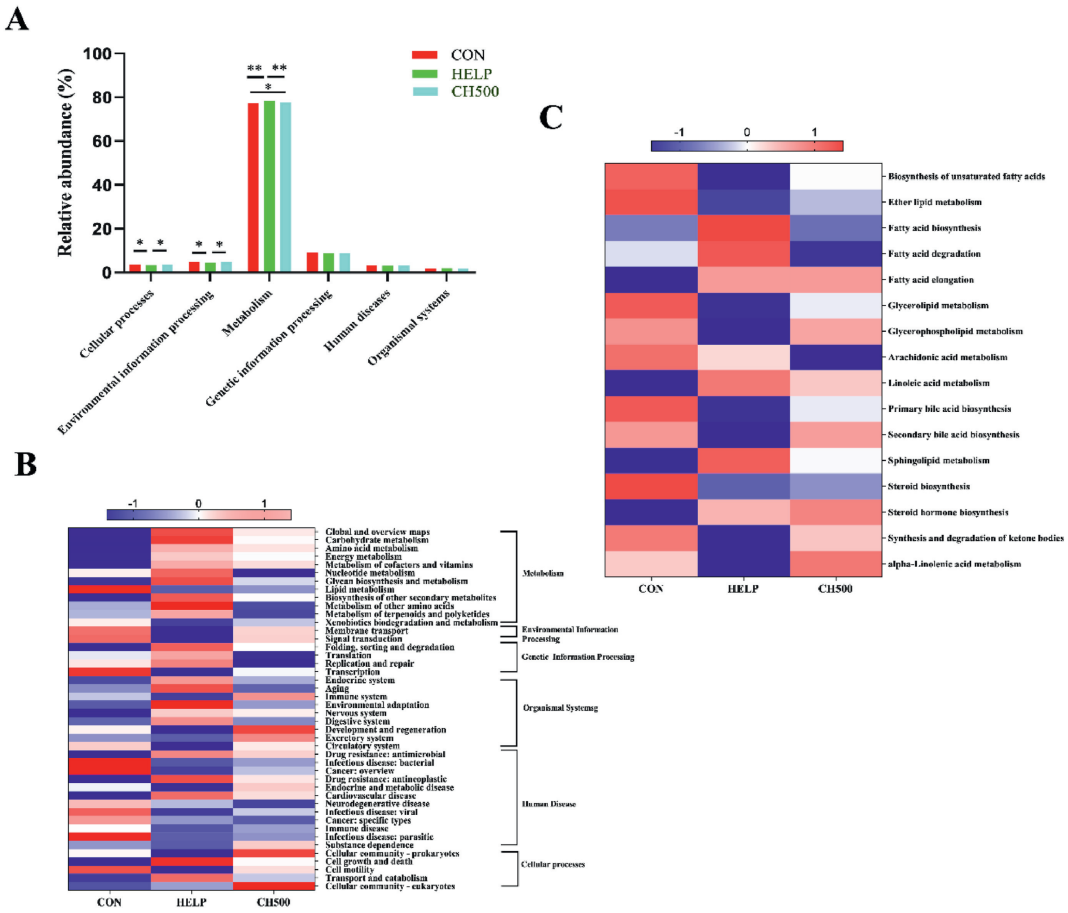

Fig. 6. Predictive analysis of intestinal flora function. (A) Predictive analysis of KEGG function in intestinal flora level 1. (B) Metabolism of intestinal flora KEGG function predictive analysis of level 2. (C) Lipid metabolism of KEGG functional predictive analysis of intestinal flora level 3. CON = normal diet; HELP = high-energy and low-protein diet; CH500 = 500 mg/kg coated sodium butyrate added to high-energy and low-protein diet. *$P < 0.05$, **$P < 0.01$.

their LPS and flagellin by interacting with cell receptors (Plöger et al., 2012). Our detailed LEfSe analysis demonstrated that the CSB-induced increase in Firmicutes phylum was associated with the rise of *unclassified_f_Oscillospiraceae, Sellimonas, norank_f_UCG-010, and norank_f_Eubacterium_coprostanoligenes_group* genera relative abundance, whereas the decrease in the Bacteroidetes phylum was mainly attributed to a reduction relative abundance of *Rikenellaceae_RC9_gut_group* genus abundance. Additionally, CSB intervention increased microbiota diversity in HELP diet-induced FLHS laying hens. A high microbiota diversity is theoretically considered to enhance the ecosystem's defense against pathogens (Konopka, 2009). These results indicated that the amelioration of CSB on intestinal barrier dysfunction and inflammatory events in HELP diet-induced FLHS laying hens may be attributed to the regulation of microbes, especially the improved Firmicutes/Bacteroidetes ratio and increased microbiota diversity. In agreement with our findings, Zhou et al. (2017) reported that sodium butyrate intervention mitigated the high-fat diet-induced decreases in Firmicutes/Bacteroidetes ratio in mice.

The gut microbiota has been reported to modulate the intestinal metabolic phenotype, including microbiota- and host-derived metabolites, and in turn affect gut homeostasis and disease (Li et al., 2016; Hu et al., 2020). Thus, the way CSB-induced microbial alterations affected the metabolic phenotype was further investigated in this study. The GC/MS analysis revealed that CSB intervention reshaped not only the gut microbiota but also the metabolic phenotype. Among the 25 identified biomarker metabolites, a notable observation was the significant decrease in the levels of metabolites associated with linoleic acid and arachidonic acid metabolism following CSB intervention. Moreover, the predicted function of the altered microbiota according to PICRUSt analysis shows that the HELP diet-induced FLHS increased linoleic acid and arachidonic acid metabolism, which was reversed by CSB intervention. Considering that the CSB-induced microbial alterations were mainly related to changes in Firmicutes and Bacteroidetes, it was intriguing to investigate whether CSB influenced the production of the above metabolites by modulating the Firmicutes/Bacteroidetes ratio. By correlation analysis, we found that most of the changed genera from Firmicutes (*Sellimonas, norank_f_UCG-010, and norank_f_Eubacterium_coprostanoligenes_group*) in the CH500 group were negatively associated with metabolites related to linoleic acid and arachidonic acid metabolism. These findings suggested that the CSB-induced Firmicutes/Bacteroidetes ratio improvement might have caused or contributed to the decrease of linoleic acid and arachidonic acid metabolite levels. However, the detailed mechanism of how those microbes are involved in the participation of linoleic acid and arachidonic acid metabolism after CSB intervention in HELP diet-induced FLHS laying hens remains to be further elucidated.

Arachidonic acid, derived from linoleic acid, represents an essential polyunsaturated fatty acid (PUFA) intricately involved in inflammatory processes within the gastrointestinal tract (Ma et al., 2021). In this investigation, linoleic acid metabolism encompassed 5 metabolites, while arachidonic acid metabolism involved 11

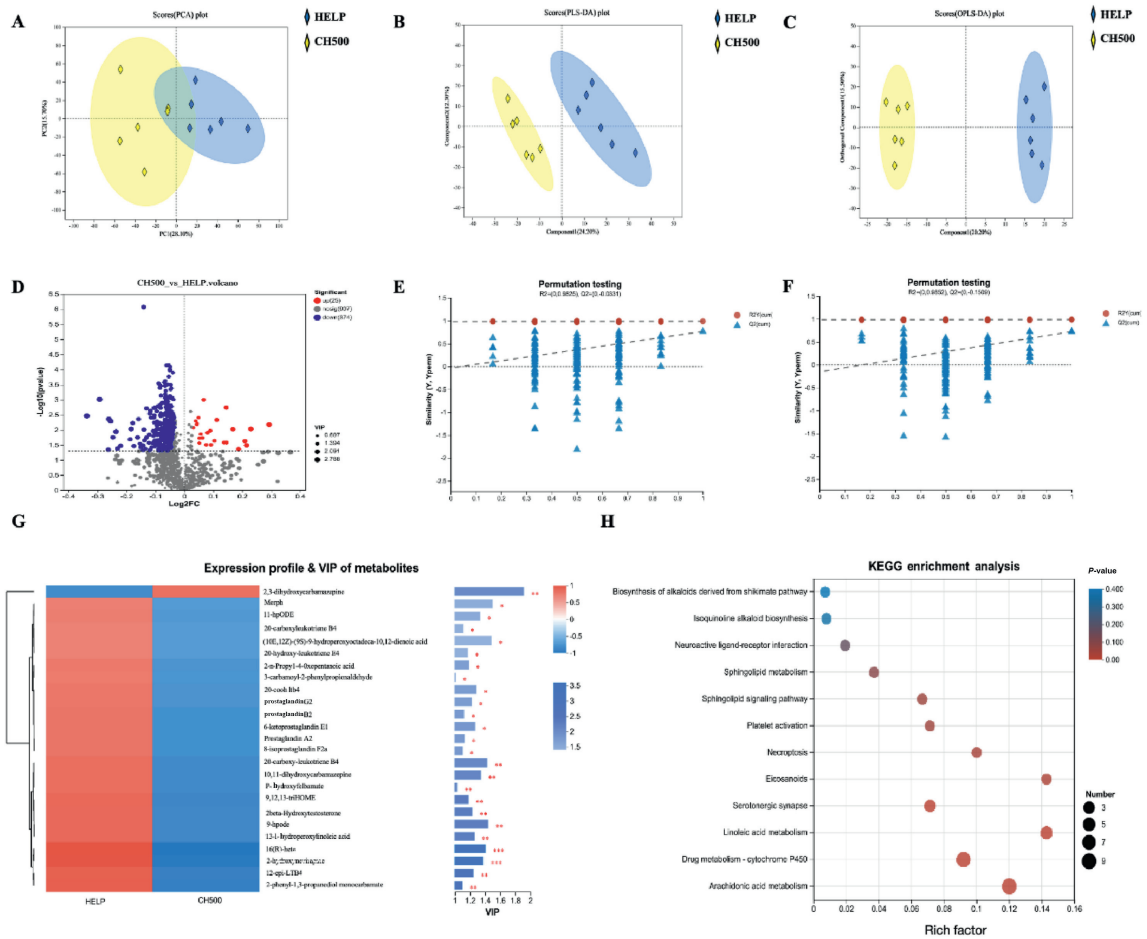

Fig. 7. Coated sodium butyrate (CSB) altered the caecal metabolome induced by high-energy and low-protein (HELP) diets in laying hens. (A), (B) and (C) score plot of principal component analysis (PCA), partial least squares discriminant analysis (PLS-DA) and orthogonal partial least squares discriminant analysis (OPLS-DA). (D) Volcano plot of differential metabolites. (E) and (F) permutation test plot of PLS-DA and OPLS-DA. The horizontal axis represents the permutation retention of the permutation test, the vertical axis represents the value of R2 or Q2, the red dot represents the value of R2Y, the blue square dot represents the value of Q2, and the two dashed lines represent the regression lines of R2Y and Q2. (G) Heatmap of hierarchical clustering analysis. The left side is the metabolite clustering dendrogram, and the right side is the metabolite variable importance projection (VIP) bar graph, the bar length indicates the value of the metabolite's contribution to the difference between the two groups, the default is not less than 1, and the larger the value indicates that the metabolite has a greater difference between the two groups. (H) KEGG enrichment analysis. The horizontal coordinate is the enrichment rate, calculated as num_in_study/num_in_pop; the vertical coordinate is the KEGG pathway. The size of the bubbles in the graph represents how much of the pathway is enriched to compounds in the metabolic set, and the color of the bubbles indicates the size of the *P*-value for different enrichment significance. HELP = HELP diet; CH500 = 500 mg/kg CSB added to HELP diet. $^{*}P < 0.05$, $^{**}P < 0.01$, $^{***}P < 0.001$.

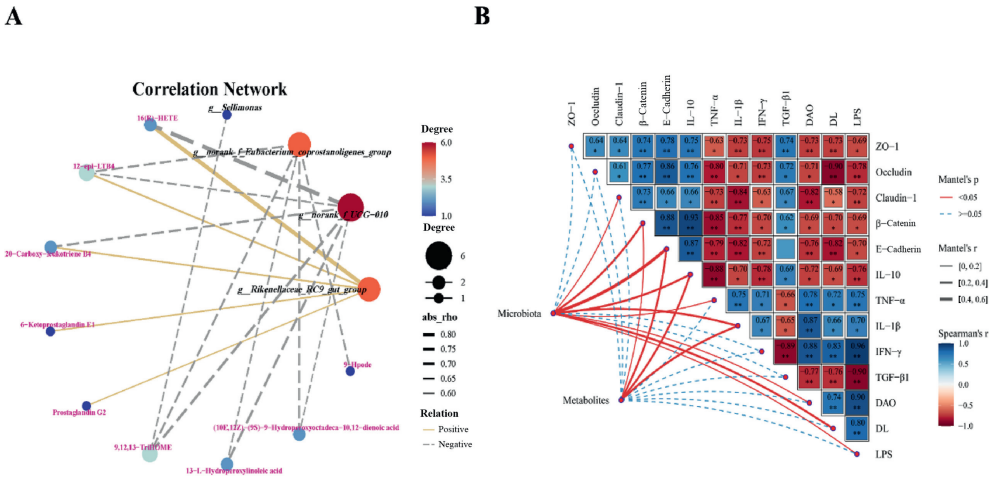

Fig. 8. Statistical Spearman's correlation between intestinal microbial genus, metabolites and intestinal barrier-related parameters. (A) Spearman correlation network was constructed to assess the associations between representative genera affiliated with Firmicutes and Bacteroidetes, and identified metabolites within arachidonic acid and linoleic acid metabolism. (B) Mantel test network heat map analysis revealed the relationships among microbial genera, metabolites and intestinal barrier-related parameters. *ZO-1* = zonula occluden-1; *IL-10* = interleukin-10; *TNF-α* = tumor necrosis factor-α; *IL-1β* = interleukin-1β; *IFN-γ* = interferon-γ; *TGF-β1* = transforming growth factor beta 1; DAO = diamine oxidase; DL = D-lactate; LPS = lipopolysaccharide. $^{*}P < 0.05$, $^{**}P < 0.01$.

metabolites. Among the linoleic acid metabolites were prostaglandins, leukotrienes, and other inflammatory mediators. Research indicated that the secretion of prostaglandin could trigger intestinal irritation and foster the development of intestinal inflammation (Mohamed et al., 2011; Leung et al., 2012). In addition, leukotrienes are well-recognized inflammatory mediators (Osher et al., 2006; Talahalli et al., 2010), and are involved in various chronic intestinal disorders, including inflammatory bowel disease (Arthur and Sundaram, 2014). In the current study, the metabolite concentrations of the arachidonic acid and linoleic acid metabolic pathways were reduced by the addition of CSB, which suggested that CSB intervention might further ameliorate the injured intestinal barrier via decreasing arachidonic acid and linoleic acid metabolites in the HELP diet-induced FLHS laying hens. Additionally, a strong correlation between intestinal barrier mediators (tight junction proteins, pro-inflammatory factors, makers of intestinal permeability), microbes (genera from Firmicutes and Bacteroidetes) and metabolites (involved in arachidonic acid and linoleic acid metabolism) was observed using Mantel-test analysis in the current study. This result complements earlier reports that intestinal microbiota and metabolic phenotype should be important modulators of intestinal barrier function (Lee, 2015; Li et al., 2018), and supports this hypothesis that gut microbes and metabolites can be denoted as potential therapeutic CSB targets for ameliorating intestinal barrier dysfunction in HELP diet-induced FLHS laying hens.

5. Conclusions

The CSB intervention could ameliorate HELP diet-induced intestinal barrier dysfunction by improvements on structural integrity, permeability and inflammatory events. These benefits are likely attributable to the modulatory effects of CSB on gut microbiota and metabolites, evidenced by the improvement of the Firmicutes/Bacteroidetes ratio and the decrease in metabolites of the linoleic acid and arachidonic acid metabolic pathway. Our findings will provide a promising strategy for the treatment of intestinal metabolic disorders by using CSB in laying hens and will contribute to the yield and safety of chicken eggs.

Credit Author Statement

Sasa Miao: Investigation, Methodology, Data curation, Formal analysis, Writing-Original draft. **Jiankui Li:** Methodology, Writing - original draft. **Ying Chen:** Investigation, Methodology, Data curation. **Wenyan Zhao:** Investigation, Methodology, Data curation. **Mengru Xu:** Methodology, Data curation. **Fang Liu:** Methodology, Data curation. **Xiaoting Zou:** Research design, Funding acquisition. **Xinyang Dong:** Research design, Funding acquisition.

Declaration of competing interest

We declare that we have no financial and personal relationships with other people or organizations that can inappropriately influence our work, and there is no professional or other personal interest of any nature or kind in any product, service and/or company that could be construed as influencing the content of this paper.

Acknowledgments

This research was supported by the Twinning Service Plan of the Zhejiang Provincial Team Science and Technology Special Commissioner (Anji County, Huzhou, China), the Science and Technology Development Project of Hangzhou (202003A02) and the Modern Argo-Industry Technology Research System of China (CARS-40-K10).

Appendix A. supplementary data

Supplementary data to this article can be found online at https://doi.org/10.1016/j.aninu.2024.06.006.

References

Abu-Shanab A, Quigley EMM. The role of the gut microbiota in nonalcoholic fatty liver disease. Nat Rev Gastroenterol Hepatol 2010;7(12):691–701.
AOAC. Official methods of analysis. 18th ed. Gaithersburg, MD: AOAC International; 2006.
Arthur S, Sundaram U. Protein kinase C-mediated phosphorylation of RKIP regulates inhibition of Na-alanine cotransport by leukotriene D(4) in intestinal epithelial cells. Am J Physiol Cell Physiol 2014;307(11):C1010–6.
Boursier J, Mueller O, Barret M, Machado M, Fizanne L, Araujo-Perez F, et al. The severity of nonalcoholic fatty liver disease is associated with gut dysbiosis and shift in the metabolic function of the gut microbiota. Hepatology 2016;63(3):764–75.
Cao S, Shen Z, Wang C, Zhang Q, Hong Q, He Y, et al. Resveratrol improves intestinal barrier function, alleviates mitochondrial dysfunction and induces mitophagy in diquat challenged piglets. Food Funct 2019;10:344–54.
Capaldo CT, Powell DN, Kalman D. Layered defense: how mucus and tight junctions seal the intestinal barrier. J Mol Med (Berl) 2017;95(9):927–34.
Csak T, Ganz M, Pespisa J, Kodys K, Dolganiuc A, Szabo G. Fatty acid and endotoxin activate inflammasomes in mouse hepatocytes that release danger signals to stimulate immune cells. Hepatology 2011;54(1):133–44.
Duarte SMB, Stefano JT, Oliveira CP. Microbiota and nonalcoholic fatty liver disease/nonalcoholic steatohepatitis (NAFLD/NASH). Ann Hepatol 2019;18(3):416–21.
Gantois I, Ducatelle R, Pasmans F, Haesebrouck F, Gast R, Humphrey TJ, et al. Mechanisms of egg contamination by salmonella Enteritidis. FEMS Microbiol Rev 2009;33(4):718–38.
Gao X, Liu P, Wu C, Wang T, Liu G, Cao H, et al. Effects of fatty liver hemorrhagic syndrome on the amp-activated protein kinase signaling pathway in laying hens. Poult Sci 2019;98(5):2201–10.
Geng S, Cheng S, Li Y, Wen Z, Ma X, Jiang X, et al. Faecal microbiota transplantation reduces susceptibility to epithelial injury and modulates tryptophan metabolism of the microbial community in a piglet model. J Crohns Colitis 2018;12(11):1359–74.
Grilli E, Tugnoli B, Foerster CJ, Piva A. Butyrate modulates inflammatory cytokines and tight junctions components along the gut of weaned pigs. J Anim Sci 2016;94(Suppl 3):433–6.
Gu W, Wen K, Yan C, Li S, Liu T, Xu C, et al. Maintaining intestinal structural integrity is a potential protective mechanism against inflammation in goose fatty liver. Poult Sci 2020;99(11):5297–307.
Hamid H, Zhang JY, Li WX, Liu C, Li ML, Zhao LH, et al. Interactions between the cecal microbiota and non-alcoholic steatohepatitis using laying hens as the model. Poult Sci 2019;98(6):2509–21.
Hu B, Ye C, Leung EL, Zhu L, Hu H, Zhang Z, et al. Bletilla striata oligosaccharides improve metabolic syndrome through modulation of gut microbiota and intestinal metabolites in high fat diet-fed mice. Pharmacol Res 2020;159:104942.
Huang C, Song P, Fan P, Hou C, Thacker P, Ma X. Dietary sodium butyrate decreases postweaning diarrhea by modulating intestinal permeability and changing the bacterial communities in weaned piglets. J Nutr 2015;145(12):2774–80.
Jeurissen SH, Lewis F, van der Klis JD, Mroz Z, Rebel JM, ter Huurne AA. Parameters and techniques to determine intestinal health of poultry as constituted by immunity, integrity, and functionality. Curr Issues Intest Microbiol 2002;3(1):1–14.
Konopka A. What is microbial community ecology? ISME J 2009;3(11):1223–30.
Le Roy T, Llopis M, Lepage P, Bruneau A, Rabot S, Bevilacqua C, et al. Intestinal microbiota determines development of non-alcoholic fatty liver disease in mice. Gut 2013;62(12):1787–94.
Lee SH. Intestinal permeability regulation by tight junction: implication on inflammatory bowel diseases. Intest Res 2015;13(1):11–8.
Leung J, Hang L, Blum A, Setiawan T, Stoyanoff K, Weinstock J. Heligmosomoides polygyrus abrogates antigen-specific gut injury in a murine model of inflammatory bowel disease. Inflamm Bowel Dis 2012;18(8):1447–55.
Li M, Shu X, Xu H, Zhang C, Yang L, Zhang L, et al. Integrative analysis of metabolome and gut microbiota in diet-induced hyperlipidemic rats treated with berberine compounds. J Transl Med 2016;14(1):237.
Li H, Gong Y, Xie Y, Sun Q, Li Y. Clostridium butyricum protects the epithelial barrier by maintaining tight junction protein expression and regulating microflora in a murine model of dextran sodium sulfate-induced colitis. Scand J Gastroenterol 2018;53(9):1031–42.
Liu L, Yin M, Gao J, Yu C, Lin J, Wu A, et al. Intestinal barrier function in the pathogenesis of nonalcoholic fatty liver disease. J Clin Transl Hepatol 2023;11(2):452–8.
Livak KJ, Schmittgen TD. Analysis of relative gene expression data using real-time 624 quantitative PCR and the 2(-Delta Delta C(T)) Method. Methods 2001;25(4):402–8.

Luther J, Garber JJ, Khalili H, Dave M, Bale SS, Jindal R, et al. Hepatic injury in nonalcoholic steatohepatitis contributes to altered intestinal permeability. Cell Mol Gastroenterol Hepatol 2015;1(2):222–32.
Ma X, Xu T, Qian M, Zhang Y, Yang Z, Han X. Faecal microbiota transplantation alleviates early-life antibiotic-induced gut microbiota dysbiosis and mucosa injuries in a neonatal piglet model. Microbiol Res 2021;255:126942.
Miao Z, Miao Z, Teng X, Xu S. Melatonin alleviates lead-induced fatty liver in the common carps (Cyprinus carpio) via gut-liver axis. Environ Pollut 2023;317:120730.
Miao S, Mu T, Li R, Li Y, Zhao W, Li J, et al. Coated sodium butyrate ameliorates high-energy and low-protein diet induced hepatic dysfunction via modulating mitochondrial dynamics, autophagy and apoptosis in laying hens. J Anim Sci Biotechnol 2024;15(1):15.
Mohamed JA, DuPont HL, Flores J, Palur H, Nair P, Jiang ZD, et al. Single nucleotide polymorphisms in the promoter of the gene encoding the lipopolysaccharide receptor CD14 are associated with bacterial diarrhea in US and Canadian travelers to Mexico. Clin Infect Dis 2011;52(11):1332–41.
Nielsen DS, Jensen BB, Theil PK, Nielsen TS, Knudsen KE, Purup S. Effect of butyrate and fermentation products on epithelial integrity in a mucus-secreting human colon cell line. J Funct Foods 2018;40:9–17.
Nii T. Relationship between mucosal barrier function of the oviduct and intestine in the productivity of laying hens. J Poult Sci 2022;59(2):105–13.
Nii T, Bungo T, Isobe N, Yoshimura Y. Intestinal inflammation induced by dextran sodium sulphate causes liver inflammation and lipid metabolism disfunction in laying hens. Poult Sci 2020;99(3):1663–77.
Nixon GF. Sphingolipids in inflammation: pathological implications and potential therapeutic targets. Br J Pharmacol 2009;158(4):982–93.
Osher E, Weisinger G, Limor R, Tordjman K, Stern N. The 5 lipoxygenase system in the vasculature: emerging role in health and disease. Mol Cell Endocrinol 2006;252(1–2):201–6.
Park JS, Lee EJ, Lee JC, Kim WK, Kim HS. Anti-inflammatory effects of short chain fatty acids in IFN-gamma-stimulated RAW 264.7 murine macrophage cells: involvement of NF-kappaB and ERK signaling pathways. Int Immunopharmacol 2007;7(1):70–7.
Plöger S, Stumpff F, Penner GB, Schulzke JD, Gäbel G, Martens H, et al. Microbial butyrate and its role for barrier function in the gastrointestinal tract. Ann N Y Acad Sci 2012;1258(1):52–9.
Rahman K, Desai C, Iyer SS, Thorn NE, Kumar P, Liu Y, et al. Loss of junctional adhesion molecule A promotes severe steatohepatitis in mice on a diet high in saturated fat, fructose, and cholesterol. Gastroenterology 2016;151(4):733–46.
Rozenboim I, Mahato J, Cohen NA, Tirosh O. Low protein and high-energy diet: a possible natural cause of fatty liver hemorrhagic syndrome in caged white leghorn laying hens. Poult Sci 2016;95(3):612–21.
Schoeni JL, Glass KA, McDermott JL, Wong AC. Growth and penetration of Salmonella enteritidis, Salmonella heidelberg and Salmonella typhimurium in eggs. Int J Food Microbiol 1995;24(3):385–96.
Shterzer N, Rothschild N, Sbehat Y, Stern E, Nazarov A, Mills E. Large overlap between the intestinal and reproductive tract microbiomes of chickens. Front Microbiol 2020;11:1508.
Stojanov S, Berlec A, Štrukelj B. The influence of probiotics on the Firmicutes/Bacteroidetes ratio in the treatment of obesity and inflammatory bowel disease. Microorganisms 2020;8(11):1715.
Talahalli R, Zarini S, Sheibani N, Murphy RC, Gubitosi-Klug RA. Increased synthesis of leukotrienes in the mouse model of diabetic retinopathy. Invest Ophthalmol Vis Sci 2010;51(3):1699–708.
Wang W, Zhao J, Gui W, Sun D, Dai H, Xiao L, et al. Tauroursodeoxycholic acid inhibits intestinal inflammation and barrier disruption in mice with non-alcoholic fatty liver disease. Br J Pharmacol 2018;175(3):469–84.
Wang H, Chen H, Lin Y, Wang G, Luo Y, Li X, et al. Butyrate glycerides protect against intestinal inflammation and barrier dysfunction in mice. Nutrients 2022;14(19):3991.
Xiong BH, Luo QY, Zheng SS, Zhao YG. Introduction of tables of feed composition and nutritive values in China (2020 thirty-first edition). China Feed 2020;21(1):87.
Xu Q, Zhao J, Jian H, Ye J, Gong M, Zou X, Dong X. Linoleic acid ameliorates intestinal mucosal barrier injury in early weaned pigeon squabs (Columba livia). J Anim Sci 2023;101:skad125.
Zhou D, Pan Q, Xin FZ, Zhang RN, He CX, Chen GY, et al. Sodium butyrate attenuates high-fat diet-induced steatohepatitis in mice by improving gut microbiota and gastrointestinal barrier. World J Gastroenterol 2017;23(1):60–75.